Archives of Biochemistry and Biophysics
Vol. 364, No. 1, April 1, pp. 42–52, 1999
Article ID abbi.1999.1106, available online at http://www.idealibrary.com on IDEAL®

Bacterial Expression and Characterization of the Ligand-Binding Domain of the Vitamin D Receptor[1]

Stephen A. Strugnell,[2] John J. Hill,[3] Darrell R. McCaslin, Bridgette A. Wiefling,[4] Catherine A. Royer,[5] and Hector F. DeLuca[6]

Department of Biochemistry, University of Wisconsin-Madison, 420 Henry Mall, Madison, Wisconsin 53706

Received September 14, 1998

The ligand-binding domain of the rat vitamin D receptor (amino acids 115–423) was expressed as an amino-terminal His-tagged protein in a bacterial expression system and purified over Ni-nitrilotriacetic acid resin and a Mono S column. The purified protein bound its ligand, 1,25-dihydroxyvitamin D_3, with high affinity, similar to that of the full-length protein. Saturation of the protein with ligand quenched 90% of the tryptophan fluorescence, consistent with the purified protein being uniformly able to bind ligand. Addition of ligand produced no change in the tryptophan fluorescence lifetime, suggesting static quenching as the mechanism of fluorescence decrease. The near-UV circular dichroism spectrum showed a large increase in signal following the addition of ligand, consistent with a change in the environment of aromatic amino acid side chains. The far-UV circular dichroism spectrum was consistent with a protein of high α-helical content. Sedimentation equilibrium experiments demonstrated that the protein formed higher-order complexes, and the distribution of the protein among these complexes was significantly shifted by addition of ligand.

Key Words: **vitamin D receptor; vitamin D; calcium; bone; steroid hormone receptors.**

The vitamin D receptor (VDR)[7] protein mediates the effects of vitamin D on bone, intestine, and other organs involved in maintenance of calcium homeostasis (1). This protein binds its ligand, 1,25-dihydroxyvitamin D_3 (1,25-$(OH)_2D_3$), with very high affinity, with a K_d of the order of 10^{-11} M (2). Binding of ligand to the receptor sets in motion a sequence of events that results in modulation of the rate of transcription of target genes (3).

The three-dimensional structure of the VDR remains unknown as does the exact mechanism by which the VDR interacts with the transcriptional machinery. Experiments with the cloned receptor in transfected cells have shown that the protein can be functionally divided into several domains, including the DNA-binding domain, near the amino terminus, and the ligand-binding domain (LBD), which occupies the carboxy-terminal portion of the protein (4). The LBD of the receptor is the focus of much investigation into how ligand binds to the receptor and how this binding affects receptor conformation. The structures of the LBDs of related receptors (the retinoic acid receptor γ (RARγ), the thyroid hormone receptor α (TRα), and the retinoic X receptor α (RXRα)) have been determined (5–7). The structures of these LBDs are similar, suggesting that they can be utilized as models for the LBD of the VDR. However, functional differences exist between the VDR and the other receptors which point to potential structural distinctions. For example, both the retinoid and thyroid hormones are bound by the nuclear receptor corepressor NCoR, which binds to a specific sequence in the LBDs of these proteins termed the CoR box.

[1] This work was supported in part by a program project grant (DK14881) from the National Institutes of Health and a fund from the Wisconsin Alumni Research Foundation.

[2] Present address: Bone Care International, One Science Court, Madison, WI 53711.

[3] Present address: ICOS Corporation, 22021 20th Ave., S.E., Bothell, WA 98021.

[4] Present address: 2 Sunnyside Street, Stoughton, WI 53589.

[5] Present address: Directeur de Recherche, Centre de Biochimie Structurale, INSERM U414, Faculte de Pharmacie, 15, ave. Charles Flahault, 34060 Montpellier CEDEX 01, France.

[6] To whom correspondence should be addressed. Fax: (608) 262-7122. E-mail: deluca@biochem.wisc.edu.

[7] Abbreviations used: VDR, vitamin D receptor; 1,25-$(OH)_2D_3$, 1,25-dihydroxyvitamin D_3; LBD, ligand-binding domain; RXR, retinoic X receptor; TR, thyroid hormone receptor; RAR, retinoic acid receptor; HAP, hydroxylapatite; Chaps, 3-[(3-cholamidopropyl)dimethylammonio]propanesulfonate; DTT, dithiothreitol; NTA, nitrilotriacetic acid.

0003-9861/99 $30.00

However, the VDR is not bound by NCoR, despite the presence of a CoR box sequence in the relevant part of the VDR (8). In addition, a recent report indicates that in order to form a stable heterodimer complex with RXR, the VDR requires a larger portion of the RXR protein than either RAR or TR (9). Thus, although the overall structural resemblance may be large, there are reasons to believe that the VDR LBD may differ in some key areas from related proteins.

In order to better understand the way in which the receptor protein binds ligand, we have expressed the LBD of the VDR (amino acid 115–423) in a bacteria. Following purification, the LBD was then characterized using a ligand-binding assay, fluorescence and circular dichroism spectroscopy, and by analytical ultracentrifugation. The ligand-binding assay was used to characterize the affinity of the LBD for ligand, to determine whether the protein had the same affinity for ligand as the full-length receptor. Fluorescence spectroscopy provides insight primarily into the environment of the tryptophan residues in a protein, due to their high intrinsic fluorescence, and has been used previously with other receptors as an indicator that the purified protein is homogeneous in its ability to bind ligand. Work with the retinoic acid receptor (10) and the RXR (6, 11) showed near-complete quenching of tryptophan fluorescence following ligand binding to these proteins. The relevance of these observations is also highlighted in the structure of the RARγ LBD (6), in which one of the two tryptophan residues was shown to be in close proximity to the β-ionone ring of bound retinoid. Postulating that the single tryptophan in the VDR LBD might also play a role in the high-affinity binding to 1,25-$(OH)_2D_3$, we examined the fluorescence properties of the LBD both in the presence and absence of ligand.

The LBDs of the other receptors that have been studied to date exhibited a high content of α helix based on circular dichroism data (10, 11), and this has been confirmed by X-ray crystallography (5, 6). The far-UV CD spectrum (200–250 nm) of the VDR LBD was examined to determine whether it was consistent with the high α helical content observed for these other receptors.

Near-UV CD spectra (250–300 nm) often exhibit signals arising from the aromatic residues which are sensitive to the detailed electronic environment of these residues (13). For this reason, the near-UV CD signal of LBD in the presence and absence of its ligand was examined to see if ligand binding altered the environment in the vicinity of the tryptophan residue of the LBD.

With the exception of the RXR, the oligomeric state of the LBDs of other receptors has not been extensively studied. The LBD of the RXR was reported to be either a monomer using equilibrium sedimentation analysis (12) or a dimer using gel filtration and laser light scattering (11) and was crystallized as a dimer (5). In contrast, the LBDs of both RAR and thyroid hormone receptors crystallized as monomers (6, 7), although the LBD of the thyroid hormone receptor was shown to migrate over a gel filtration column as a mixture of monomer and dimer (14). We have examined the VDR LBD by sedimentation equilibrium to determine whether the protein self-associates in solution and to see if addition of ligand to the protein has any effect upon this association.

MATERIALS AND METHODS

Construction of the bacterial expression vector. Construction of the vector for LBD with an N-terminal 6 × His tag was carried out as follows: the *Stu*I–*Bgl*II fragment of the rat VDR was excised from the expression vector pCKR3, purified on a 0.8% agarose gel, and eluted using Geneclean (Bio101). The purified DNA fragment was subcloned into the vector pET14B (Novagen, Madison, WI) in which the original *Bgl*II site had been disrupted by insertion of an oligonucleotide with *Bam*HI ends and into which a new multiple cloning site had been inserted by subcloning of an annealed duplex oligonucleotide into the *Bam*HI site. This new multiple cloning site was based on that of the vector pGEX-4T-3 and included a *Bgl*II site immediately 3′ of the stop codons. The modified vector was digested with *Sma*I and *Bgl*II and dephosphorylated with calf intestine alkaline phosphatase prior to ligation. Plasmids obtained after transformation of competent JM105 cells and overnight growth were subjected to digestion with *Bam*HI and *Bgl*II to confirm the presence of the insert.

Expression of the VDR LBD. Bacteria of the strain BL21(DE3) pLysS (Novagen) were transformed with the LBD expression vector and plated on LB agar plates containing 100 μg/ml ampicillin and 30 μg/ml chloramphenicol. After overnight growth at 37°C, an isolated colony was used to inoculate 100 ml of LB medium containing 100 μg/ml ampicillin and 30 μg/ml chloramphenicol. Following overnight growth at 37°C, 10 ml of this culture was used to inoculate 1 liter of LB medium. The cells were grown to an OD_{600} of 0.6 at 37°C and then moved to a shaker at 22°C. Protein expression was induced by addition of 0.4 mM isopropyl β-D-thiogalactoside and the cells were grown for an additional 3 h before being harvested by centrifugation. The pellets were resuspended in 10 ml/liter of 50 mM sodium phosphate buffer, pH 8.0. Phenylmethylsulfonyl fluoride was added in ethanol to a final concentration of 1 mM, followed by addition of 100 μg/ml lysozyme. After incubation at room temperature for 10 min, Tween 20 was added to a final concentration of 1%, and the cell suspensions were frozen in liquid nitrogen.

Purification of the LBD protein. The frozen cell suspensions containing the expressed LBD were thawed at room temperature, placed on ice and subjected to 5–10 bursts of sonication (30 s per burst) using a Branson sonicator equipped with a probe (VWR, Batavia, IL). The cell lysate was centrifuged at 30,000*g* for 20 min and the supernatant carefully decanted. The supernatant was applied to a column of Ni-NTA agarose (Qiagen, Santa Clarita, CA) and washed with increasing concentrations of imidazole in 50 mM sodium phosphate buffer, pH 7.0. β-Mercaptoethanol was added to a final concentration of 5 mM as an antioxidant. Purified LBD protein was eluted with a step gradient of 100–200 mM imidazole in 50 mM increments. Fractions containing the purified protein were pooled and dialyzed against 50 mM sodium phosphate buffer to remove imidazole and then further purified on a MonoS HiTrap column (Pharmacia, Piscataway, NJ) and eluted using increasing concentrations of sodium chloride from 50 to 500 mM. Purified protein fractions were pooled, dialyzed against the buffer to be used in experiments (50 mM Hepes,

pH 7.5 containing 100 mM NaCl), concentrated, and drop-frozen in liquid nitrogen.

Measurement of ligand-binding affinity. The ligand-binding affinity of the LBD was measured by a modification of the hydroxylapatite (HAP) assay. The purified LBD protein was serially diluted in 50 mM Tris–HCl, pH 7.5, containing 150 mM KCl, 100 μg/ml purified bovine serum albumin, 1% CHAPS, and 5 mM DTT. Increasing concentrations of tritiated 1,25-$(OH)_2D_3$ (160 Ci/mmol) were added to the protein, and after incubation on ice for 16 h, HAP resin (Bio-Rad, Hercules, CA) was added to bind the LBD protein and any associated ligand. This was followed by extensive washing with 50 mM Tris/1.5 mM EDTA/0.5% Triton X-100 to remove free ligand. The amount of bound ligand was quantitated by scintillation counting. Binding curves were analyzed using the program BIOEQS (15–17). This program uses a numerically based constrained optimization and thus does not require a closed-form analytical expression for the binding isotherm (18). The model used assumed ligand binding to monomeric species only and included as species free monomeric receptor, free ligand, and receptor bound ligand. BIOEQS solves the system of free energy equations for this model with the constraints of mass conservation for both protein subunits and ligand in terms of the species concentration vector. Best fit values of the free energy parameters are in turn obtained using a Marquardt–Levenberg nonlinear least squares algorithm.

Measurement of tryptophan fluorescence. All fluorescence measurements were carried out using protein concentrations between 1.0 and 5.0 μM in a buffer containing the following molecular biology grade reagents (Research Organics, Inc., Cleveland, OH): 250.0 mM Tris, 1.0 mM EDTA, 15% glycerol (spectroscopic grade; Aldrich, Milwaukee, WI), 5.0 mM DTT, and 100 mM NaCl at pH 7.6 (TEGD100).

Steady-state fluorescence emission spectra were performed using an ISS Koala automated spectral acquisition unit (ISS, Inc., Champaign, IL) with excitation from a xenon arc lamp and the excitation monochromator set at 295 nm. The excitation and emission band widths were 8 nm.

Time-resolved measurements were performed in the frequency domain using ISS frequency domain acquisition electronics. The excitation light was at 295 nm from the frequency doubled output of a coherent cavity dumped, R6G, picosecond, 701 dye laser (Coherent Corp., Palo Alto, CA) excited with the 532 line of a coherent frequency doubled mode-locked ND-YAG Antares laser (Coherent Corp.) The reference lifetime compound was paraterphenyl with a lifetime of 1.0 ns in cyclohexane (19).

Data were analyzed with the global analysis software developed by Beechem and coworkers (20), Globals Unlimited (LFD, Urbana, IL).

Sedimentation equilibrium studies. Sedimentation equilibrium experiments were conducted in a Beckman XL-A analytical ultracentrifuge. To reduce interference from the absorbance of oxidized DTT at 280 nm, the purified protein was dialyzed into fresh experimental buffer (50 mM Hepes/100 mM NaCl/0.1 mM DTT, pH 7.5). Samples with varying initial concentrations (0.6 to 2 mg/ml) were run at 4°C at several rotor speeds in an An60 rotor. Equilibrium was verified by comparing gradients approximately 2 h apart until no further change in the profile was observed. The presence of nonsedimenting absorbance was determined by high-speed sedimentation to deplete all protein species. Sedimentation equilibrium data were fit by nonlinear least squares curve fitting (using Igor Pro; Wavemetrics, Lake Oswego, OR) to various models that included one, two, or three thermodynamically ideal species in a manner similar to that discussed in Laue (21). The data were also examined in plots of ln(absorbance) vs radial distance squared. In these plots the slope at any point (after correction of nonsedimenting material) is proportional to the weight average molecular weight of the mixture of species present.

The partial specific volume of LBD used was 0.732 ml/gm calculated from the amino acid composition described by Cohn and Edsall (22). The monomer weight based on sequence is 37,400. The solvent density was 1.0 g/ml. At 280 nm, a solution of LBD of 1 mg/ml (based on Bradford protein assay using BSA as standard) gave an absorbance of 0.41 for a 1-cm path length. This corresponds to an extinction coefficient of 15,000 M^{-1} cm^{-1}.

Measurement of circular dichroism spectra. Samples of the purified LBD protein were diluted to 0.2 mg/ml in Hepes/NaCl/DTT buffer and the circular dichroism spectra were recorded on an Aviv 62A DS circular dichroism spectrophotometer equipped with a thermoelectric temperature control unit (Aviv Instruments, Lakewood, NJ). Spectra in the far-UV region were recorded in 0.1-cm-path length quartz cuvettes at 25.0°C. The buffer blank was recorded under the same conditions and subtracted from the sample signal. Thermal denaturation was monitored at 207 nm, with temperature scanned from 25 to 85°C in 5°C increments. The signal was recorded immediately upon temperature stabilization as detected by the CD software. CD spectra of the thermally denatured protein were recorded at both 25 and 85°C.

The CD signal of the protein in the near-UV portion of the spectrum (250 to 300 nm) was recorded at 25°C using a protein concentration of 2.0 mg/ml, in a 1-cm-path length masked quartz cuvette. Ligand was added in small aliquots and the contents of the cuvette were mixed by repeated pipetting.

RESULTS

SDS–PAGE analysis of the purified LBD is shown in Fig. 1. Following elution from the Ni-NTA column (Fig. 1A), the protein was judged to be approximately 85% pure. After further purification on the MonoS column, the protein was judged to be greater than 95% pure (Fig. 1B). The ligand-binding affinity of the purified protein was measured by a modification of the HAP-binding assay and the results are shown in Fig. 2. The program BIOEQS (see Materials and Methods) was used to fit the data (solid line) and gave a dissociation equilibrium constant, K_d, of 0.3 nM.

The fluorescence emission spectra of the LBD in absence and presence of 1,25-$(OH)_2D_3$ are shown in Fig. 3. It can be seen that addition of sixfold excess ligand produces a near 90% loss in the tryptophan's emission intensity. Figure 4 shows that a titration of the receptor with ligand produces saturation at a 1:1 complex and that the maximum change in intensity is approximately 90%. 1,25-$(OH)_2D_3$ has a nominal absorption at the 295-nm excitation wavelength, and the intensity decrease is maximum at a 1:1 complex (Fig. 4), which suggests that the intensity loss is not an inner filter effect. There is no significant change in the UV absorption spectrum of LBD after addition of a saturating amount of ligand and adjustment for the ligand's absorption (data not shown), indicating that the decrease in emission intensity is not due to a change in the tryptophan's extinction coefficient.

To determine the nature of the emission decrease the frequency response of the LBD tryptophan (295-nm excitation) was obtained at multiple emission wavelengths (Fig. 5). Simultaneous analysis of the data at all wavelengths was performed using a triple exponential decay and a linkage scheme in which the three

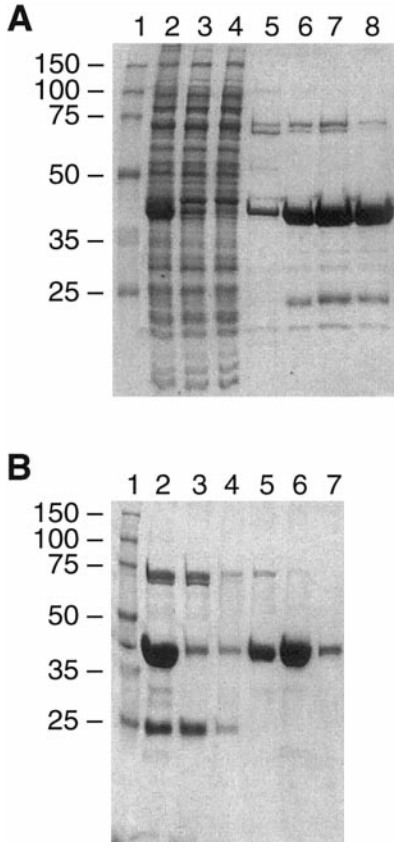

FIG. 1. Purification of the LBD protein. The LBD domain of the rat VDR (amino acids 115–423) was purified from bacterial extract over nickel resin, followed by cleanup over a MonoS column. (A) Purification over Ni-NTA resin. Lane 1, perfect protein markers; lane 2, crude bacterial lysate; lane 3, cleared supernatant after centrifugation; lane 4, flowthrough from the Ni-NTA column; lane 5, 50 mM imidazole eluate; lane 6, 100 mM imidazole; lane 7, 150 mM imidazole; lane 8, 200 mM imidazole. (B) Further purification of Ni-NTA eluates over MonoS. Lane 1, perfect protein markers; lane 2, pooled Ni-NTA eluates; lane 3, flowthrough from the MonoS column; lane 4, buffer wash; lane 5, 50 mM NaCl wash; lane 6, 100 mM NaCl; lane 7, 200 mM NaCl.

lifetime components across the emission spectrum were considered to be the same in all data sets, while the fractional component to the total intensity (f_i) was allowed to vary across the spectrum. Decay-associated spectra, shown in Fig. 6, were obtained by multiplying the fractional intensities, f_i, for a given component recovered from the analysis for a given emission wavelength by the total steady-state emission intensity at that wavelength. Table I provides a summary of this analysis and illustrates that the three lifetime values recovered from the linked analysis are the same, within error in the absence or in the presence of ligand. The slight change in fractional populations between the 3- and 7-ns values, upon addition of ligand, cannot account for the 90% loss in intensity. Therefore, the addition of ligand produces no significant effects upon the tryptophan's lifetimes or its fractional populations as a function of wavelength, suggesting that the intensity losses are due to static quenching.

The far-UV CD spectrum of native LBD at 25°C is shown in Fig. 7. The shape of the spectrum shows the characteristic double minima at 220 and 207 nm, consistent with a high content of helical structure, as might be anticipated by comparison with LBDs of related structures. Using the methods of Greenfield and Fasman (23), Chen *et al.* (24), and the neural network approach of Andrade *et al.* (25), the helical contents of native LBD were estimated as 23.2, 20.0, and 26%, respectively. When saturating amounts of ligand were added, a slight increase in the magnitude of the ellipticity at around 220 nm is observed, which remains to be more fully examined. Thermal denaturation of LBD was found to be irreversible; the spectrum of thermally denatured LBD at 25°C is shown in Fig. 7. The spectrum at 85°C was similar in shape but somewhat reduced in magnitude. These spectra are quite distinct from that of the native LBD and suggest the loss of helical structure during the denaturation process. Using the predictive schemes mentioned above, the helical content decreased to 11, 10, and 21%, respectively. The temperature for half-maximal loss of signal at 207 nm was dependent on the details of the temperature scan, and was approximately 55°C when the signal was recorded immediately upon temperature equilibration and at 5°C increments.

The CD signal of the protein in the near-UV portion of the spectrum (250 to 300 nm) was also examined. The spectrum of LBD in absence of ligand exhibited a very small signal throughout the range of 250–300 nm (Fig. 8), with small positive peaks at approximately 258 and 265 nm. Addition of ligand resulted in major changes in the shape of the spectrum especially near 277 nm, where a large negative peak is established. Ligand itself had a very small signal in this spectral region, negligible up to 280 nm and slightly positive above and negative below this wavelength; the magnitudes of the ligand signal itself would not approach the observed signal at any of the concentrations used in Fig. 8 (data not shown). Thus, the binding of ligand induces a broad, strong negative peak in the near-UV CD spectrum. The small peaks at 258 and 265 nm appear to remain and to be superimposed on this feature. This increase was saturable at approximately a 1:1 ratio of ligand to protein, indicating that once all available binding sites were occupied, no additional signal was generated by excess ligand.

The state of association of the LBD in solution was examined by sedimentation equilibrium. In fitting data such as in Fig. 9A, we allow the inclusion of a nonsedimenting (baseline) component in addition to the molecular characteristics of the sedimenting species and their interactions. Models that yield baselines substan-

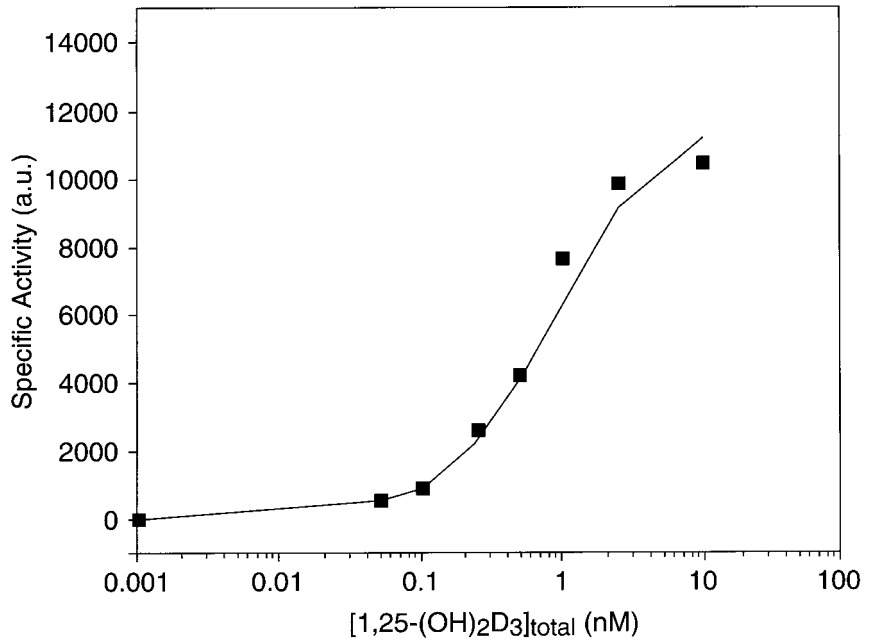

FIG. 2. Ligand-binding affinity of the purified LBD protein. Protein eluted from the MonoS column was diluted and incubated with tritiated ligand overnight at 4°C in 50 mM Tris/100 mM KCl/5 mM DTT/0.5% Chaps, pH 7.5. Ligand bound to protein was extracted using HAP resin and quantitated using scintillation counting.

tially different from that determined by high-speed depletion of the protein are judged as incorrect. Fitting data such as in Fig. 9A as single species invariably yields molecular weights intermediate between that of the monomer and dimer and yields baselines substantially higher than those observed experimentally. We attempted to fit equilibrium gradients for LBD in the absence of ligand at various speeds and initial concen-

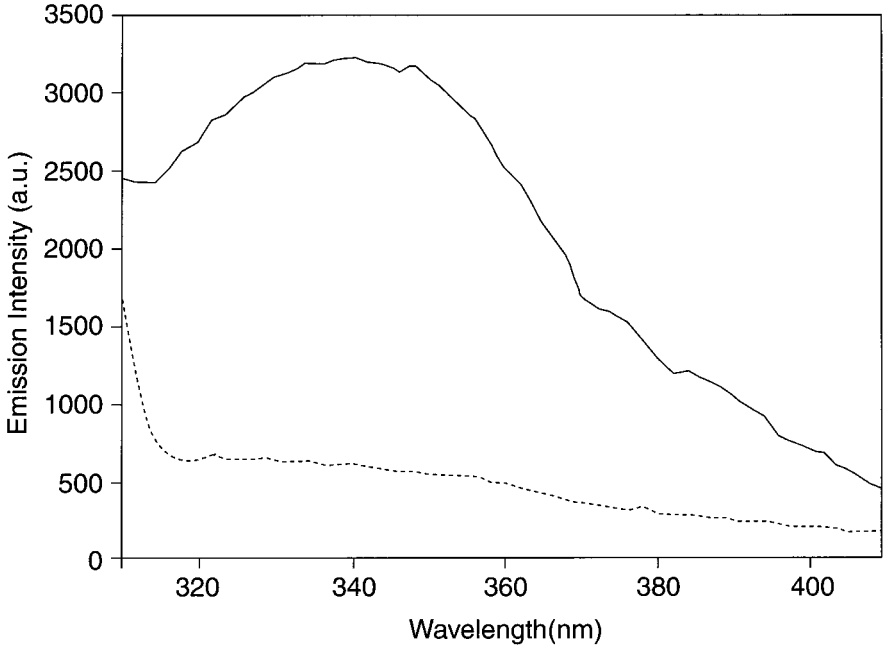

FIG. 3. Fluorescence emission spectra of purified LBD protein in the absence (solid line) and presence (dashed line) of 18 μM ligand with an excitation wavelength of 295 nM. An LBD protein concentration of 2.6 μM in 50 mM Tris/100 mM NaCl/1.0 mM EDTA/5 mM DTT/15% (w/v) glycerol, pH 7.5, buffer at 21°C and a quartz, semi-micro fluorescence cell with a 1-cm path were used.

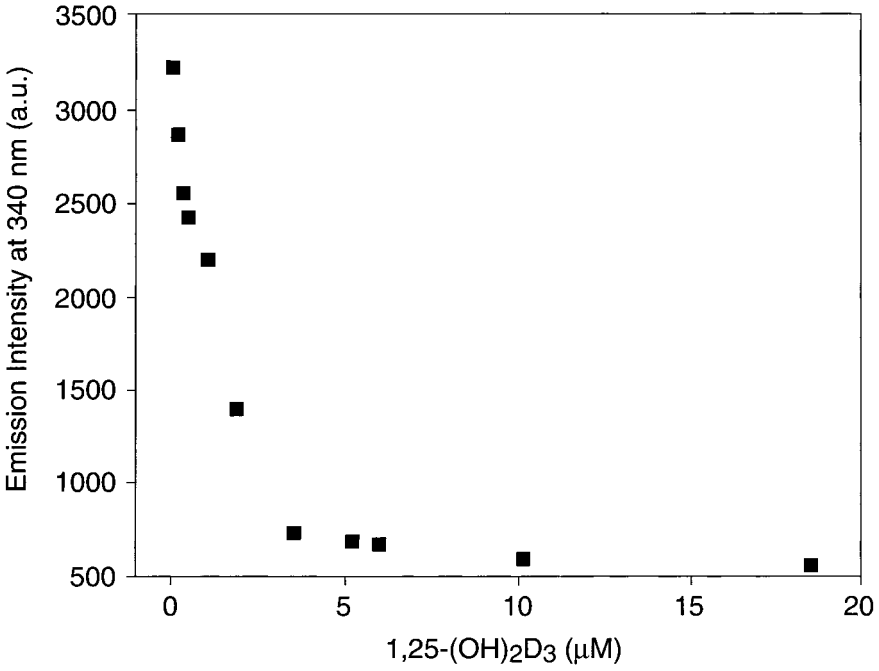

FIG. 4. Stoichiometric titration of 2.6 μM LBD protein with ligand, monitored by tryptophan fluorescence emission quenching at 340 nm. Conditions were the same as those described in the legend to Fig. 3.

trations, individually and globally, to models containing different numbers of species and whether the species were in equilibrium or not. The results have not yielded consistent results across all data sets, as the weights of smallest species present usually came out intermediate between that of the monomer and dimer and with baselines substantially different than the experimentally observed values. When LBD was allowed to reach sedimentation equilibrium and then the speed was reduced to one used earlier in the experiment, we observed that the absorbance at equilibrium at the lower speed at any point in the cell was lower than the original data. This suggests that at the high speed, LBD has formed large aggregates that either do not or only slowly disaggregate. The formation and presence of such aggregates are likely one of the factors complicating the curve fitting of the sedimentation. Thus, we do not at this time have enough information to fully define the molecular species distribution of LBD in solution.

Plots of In(absorbance) vs radial position squared after correcting for the nonsedimenting baselines as in Fig. 9B permit us to gain some insight into the nature of species present in any given sedimentation equilibrium gradient. The slope of the curve at any point is directly proportional to the weight average molecular weight of all species present at that radial position and total concentration (absorbance). The curvature in the plots in Fig. 9B immediately suggests the presence of multiple species of LBD in solution. In these data the curve at low initial protein concentration shows more curvature than does the higher initial concentration. The slope at low values of radial position in the absence of ligand corresponds to weight average molecular weights of 49,900 and 56,600 for the low and high initial concentrations, respectively. Both of these numbers are larger than the monomer molecular weight based on sequence (37,400) and smaller than that expected for the dimer. Since the weights at the highest radial position were 87,800 and 79,100, the presence of species larger than the dimer can be inferred and may include the large aggregates discussed as well as other species. Thus, the data implicate at the least the presence of monomeric LBD and higher oligomers.

The effect of ligand addition upon the oligomeric state of the LBD was also examined. Examples of sedimentation equilibrium data at two different initial concentrations of protein each in the presence and absence of saturating amounts of ligand are shown in Fig. 9. The difference in curvature of the plots with ligand compared to those in the absence of ligand in Fig. 9B shows that binding of ligand generates a broader range of weight average molecular weights than are seen for the protein alone. At low values of radial position for the low initial protein concentration, the slopes with and without ligand give weight average molecular weights of 51,500 and 49,900, respectively. In both cases the presence of monomer is necessary to explain the observed values, and it seems likely that the same species must be present in both cases. How-

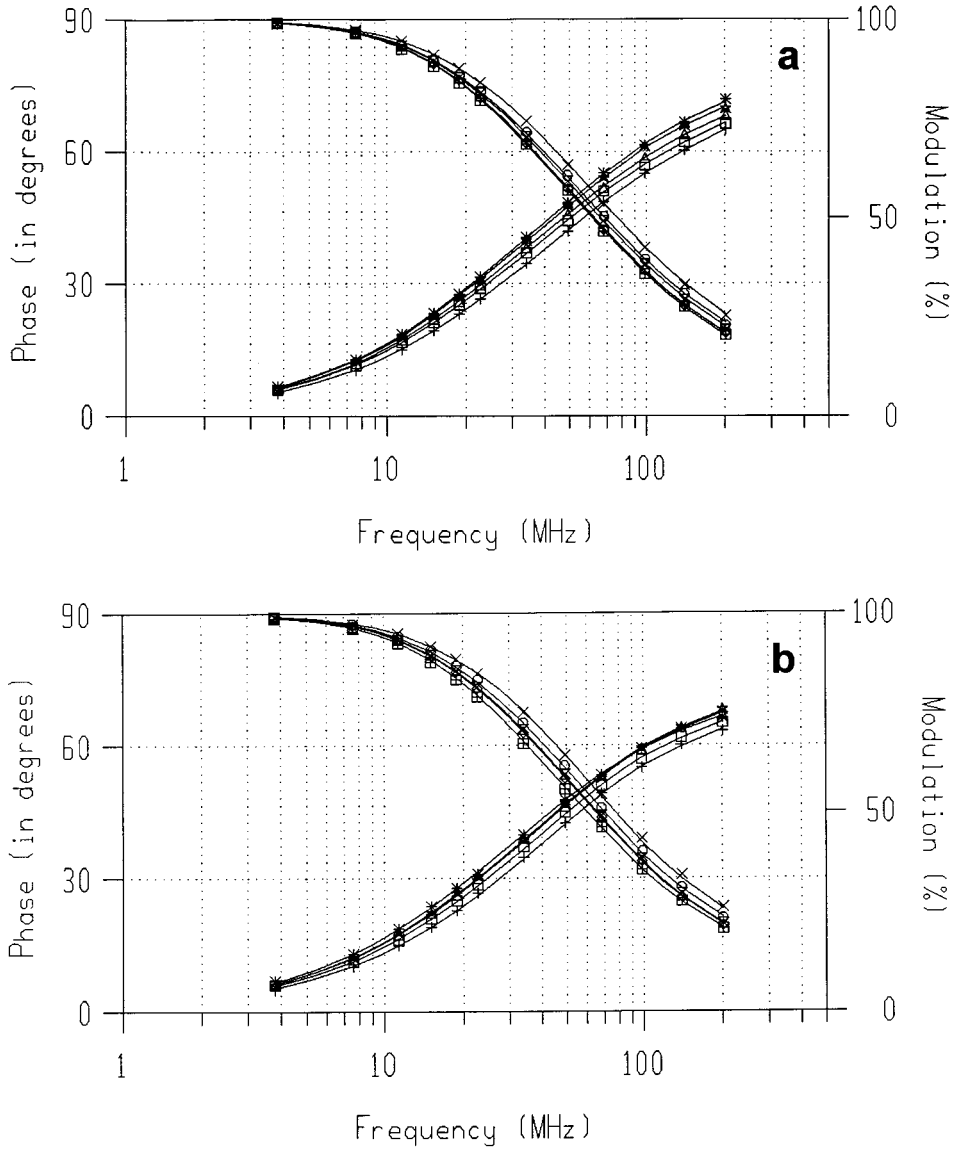

FIG. 5. Frequency responses of fluorescence at multiple emission wavelengths of 5.0 μM LBD protein in both the absence and presence of 18 μM ligand. Other conditions were the same as those described in the legend to Fig. 3.

ever, at the higher radial positions, the slope in the presence of ligand gives a molecular weight of 168,000, substantially larger than the molecular weight discussed in the previous paragraph. In the case of the higher initial concentration, the weights at all radial positions are higher in the presence of ligand than in its absence. In the presence of ligand and higher initial protein concentration, low radial positions give a weight of 66,000 and at the highest radial position, 208,000.

DISCUSSION

The ligand-binding affinity of the bacterially expressed LBD reported in this paper falls in the middle of values published for the VDR; the full-length receptor has been reported to have K_d values ranging from 0.01 nM (2) to 0.7 nM (26), when the full-length protein was expressed in baculovirus, while the LBD has been expressed in bacteria as a *S*-glutathione transferase fusion protein (27, 28) with a K_d of 0.17 nM. The reason for the variation in K_d values is unclear; it may reflect genuine differences in the affinity of the bacterially expressed protein for ligand compared to protein expressed in baculovirus or mammalian cells. Receptor made in bacteria may lack posttranslational modifications which increase the affinity of the protein for ligand. Alternatively, proteins present in eukaryotic cells may be required for the tighter binding observed

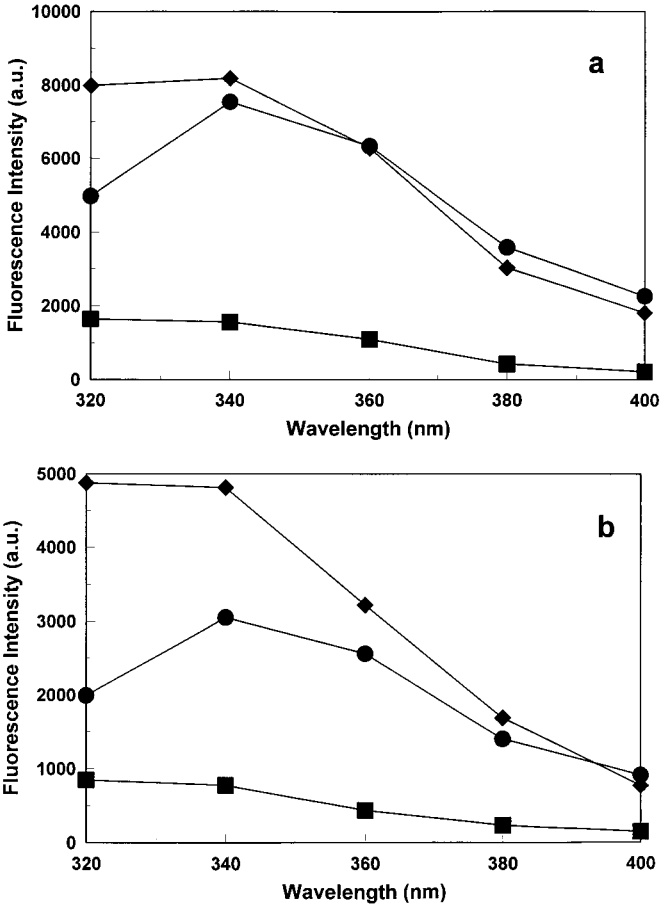

FIG. 6. Decay-associated spectra of 5.0 μM LBD protein in both the absence and the presence of 18 μM ligand. Other conditions were the same as those described in the legend to Fig. 3.

in these cells (29). A third possibility is that the variation is due to artifacts in the methodology; for instance, it has been noted for the RXR that the calculated percentage of protein which binds ligand varies widely with the assay used (30).

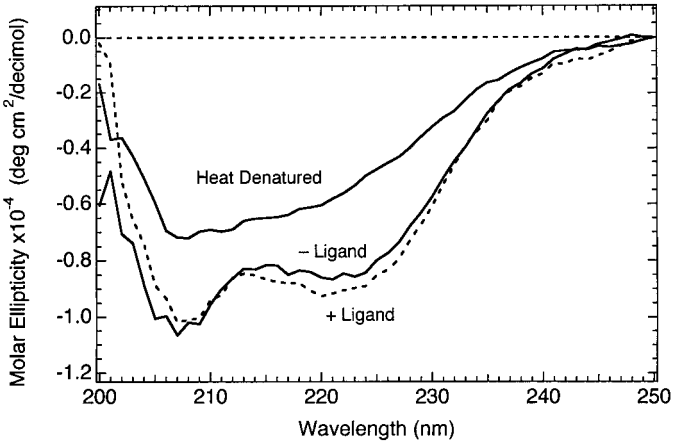

FIG. 7. Far-UV CD spectrum of LBD. Spectra were recorded at 25°C in a 0.1-cm-path length curvette at a protein concentration of 0.1 mg/ml. The heat-denatured spectrum is after heating the sample to 85°C and then cooling to 25°C. (A spectrum recorded at 85°C is similar in shape but slightly reduced in magnitude.) The dotted line is LBD in the presence of a saturating amount of ligand.

Sedimentation equilibrium studies of the LBD demonstrate that LBD exists as a mixture of species in solution, and that the smallest species present must be monomeric. More work is necessary, however, to enumerate what species are present and the molecular mechanism by which they are formed. The presence of multimers of LBD was somewhat surprising given the other receptor LBDs, such as the RAR, have not been reported to self-associate. However, as noted, the LBD of the thyroid hormone receptor was observed to behave as a mixture of monomers and dimers on a gel-filtration column (15). Although there is one conflicting report (30), most of the data concerning the RXR LBD supports the formation of dimers, including the crystal structure, gel-filtration chromatography, and dynamic light scattering (11).

Addition of ligand to LBD dramatically altered the distribution of species detected by sedimentation equi-

TABLE I

Decay Associated Spectra—Global Analysis Results

Sample	Emission λ (nm)	f_1	τ_1 (ns)	f_2	τ_2 (ns)	f_3	τ_3 (ns)
(−) 1,25-$(OH)_2D_3$	320	0.341	6.80	0.547	2.90	0.111	0.66
	340	0.435	6.80	0.472	2.90	0.092	0.66
	360	0.464	6.80	0.460	2.90	0.076	0.66
	380	0.511	6.80	0.432	2.90	0.057	0.66
	400	0.529	6.80	0.423	2.90	0.048	0.66
(+) 1,25-$(OH)_2D_3$	320	0.259	7.06	0.635	3.13	0.107	0.54
	340	0.354	7.06	0.558	3.13	0.088	0.54
	360	0.411	7.06	0.518	3.13	0.071	0.54
	380	0.422	7.06	0.510	3.13	0.068	0.54
	480	0.503	7.06	0.422	3.13	0.075	0.54

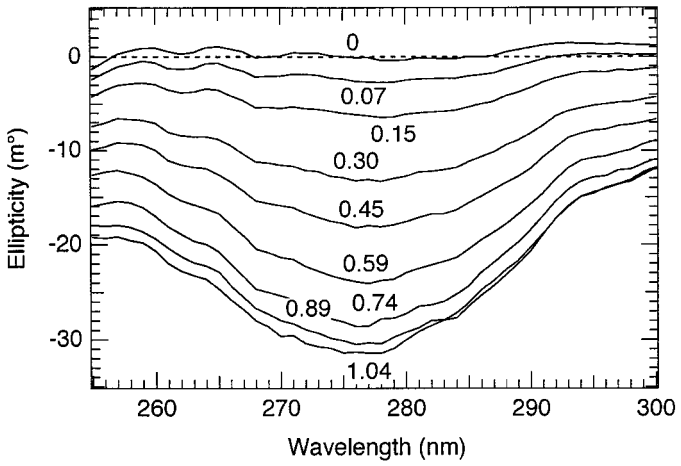

FIG. 8. Changes in near-UV CD signal upon addition of ligand to LBD. Spectra were recorded at 25°C in a 1-cm-path length cuvette at a protein concentration of 54 μM. The spectra are corrected for the buffer baseline. The numbers indicate the molar ratio of ligand to LBD.

librium (Fig. 9). While the weight average molecular weights observed at low radial positions were similar to the presence and absence of ligand, suggesting a similar mixture of species including monomer, at higher radial position (protein concentration), the apparent molecular weights in the presence of ligand were substantially higher than in the absence. This suggests that binding of ligand causes the formation of higher oligomeric states not present in the absence of ligand, or at least a shift toward higher oligomers. Alternatively, binding of ligand may limit the irreversible formation of large aggregates inferred from the work with LBD alone and result in a new distribution of species. More work is needed to define and quantitate the number of species present and their interrelationships.

The physiological significance of multimer formation for the LBD of the VDR is unclear. These data may reflect relatively nonspecific interactions between LBD monomers at the protein concentrations used, perhaps due to hydrophobic interactions between nonpolar amino acids in the ligand-binding site of the protein. In the absence of ligand, such interactions could account for the presence of large irreversible aggregates inferred from the sedimentation equilibrium studies. It has been noted previously that addition of ligand to the thyroid hormone receptor decreased the hydrophobicity of the protein (14). If the VDR LBD behaves in a similar fashion upon binding of ligand, this would decrease the extent of these hydrophobic interactions, limiting the formation of very large irreversible aggregates and shift the observed distribution to smaller oligomers but still larger than those seen in the absence of ligand. The addition of ligand to VDR has been shown to enhance its ability to heterodimerize with RXR on a response element (31, 32), and the shift among oligomeric states in LBD in response to ligand binding may reflect these interactions. However, it is possible that multimer formation by the LBD occurs through a different region of the protein than that which is involved in heterodimer formation with RXR. Alternatively, the truncated protein may act in a different manner in solution from the full-length protein, due to the absence of regions in the DNA-binding do-

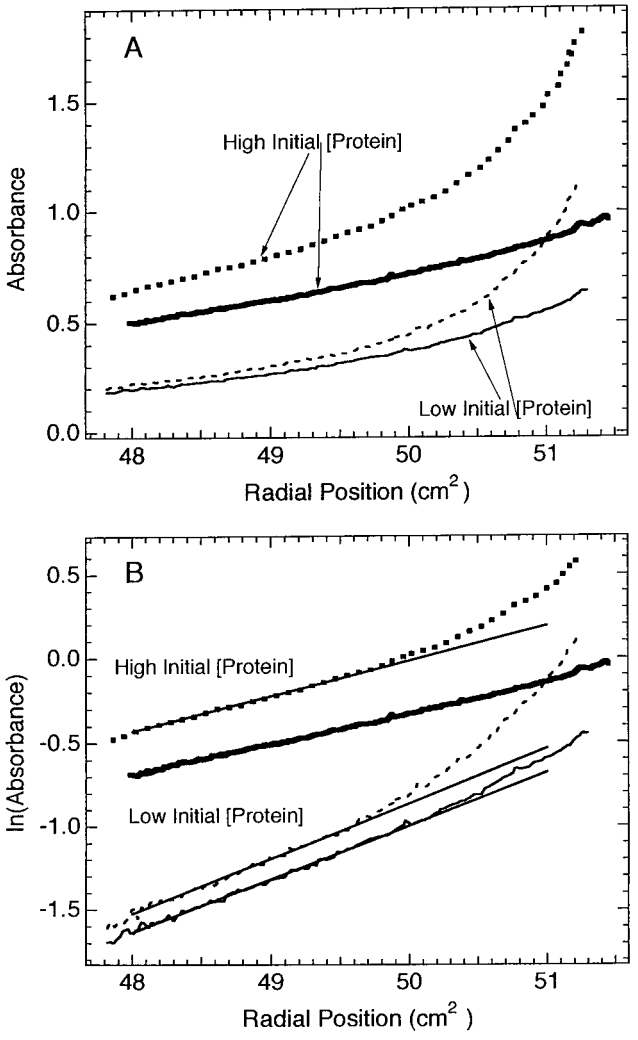

FIG. 9. Sedimentation equilibrium of native LBD. Purified protein was dialyzed into 50 mM Hepes/100 mM NaCl/0.1 mM DTT, pH 7.5. All experiments were at 4°C. Dashed lines are data in the presence of ligand, solid lines in the absence. Heavy lines are for an initial protein concentration of 0.71 mg/ml at 7000 rpm; light lines are for an initial concentration of 1.38 mg/ml at 10,000 rpm. All data are corrected for the nonsedimenting absorbance after high-speed depletion of the protein (0.039 without ligand and 0.0920 with ligand at high protein; 0.034 without and 0.060 with ligand at the low protein concentration). The ratios of ligand/protein were 1.5:1 in both samples. The straight lines originating at low radial position are the best fit lines for this region.

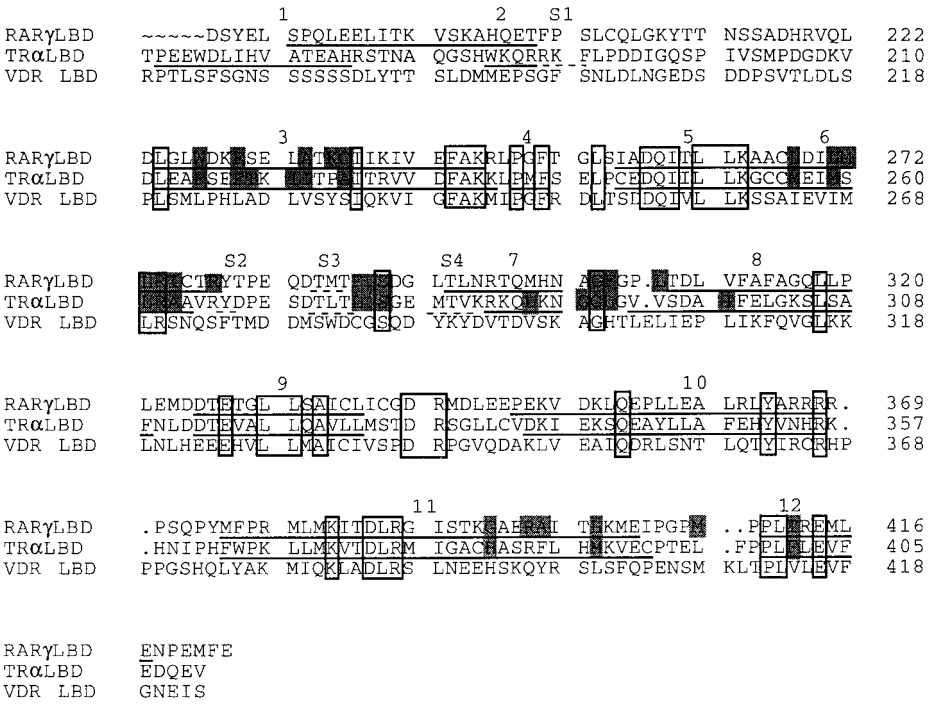

FIG. 10. Sequence alignment of the human RARγ, rat TRα, and rat VDR. The sequences of the LBDs of these proteins were aligned using the program "Pileup" (Genetics Computer Group, University of Wisconsin-Madison). Gaps introduced into the sequence to optimize the alignment are denoted by dots. Numbering of the amino acids of each LBD is to the right of the sequences and corresponds to the numbering of the full-length protein. α-helical regions of the RAR and TR are underlined with solid lines; beta-sheet regions are underlined with dashed lines. Regions of amino acid identity are enclosed with boxes. Helices are denoted by numbers in accordance with the TR structure; sheet regions are denoted s1–s4, also according to the TR structure. Amino acids in the RAR and TR shown by X-ray crystallography to be in contact with ligand are shaded.

main which modulate the behavior of the receptor. Further information on these interactions will be best gathered using full-length versions of the receptor.

One of the interesting implications of the work reported here concerns the ligand-binding conformation change of the LBD. This model of conformational change was proposed by Renaud *et al.* (6) for the RAR. The LBD of RXR (without ligand) and the RAR (with ligand) were observed to have similar secondary structures but ligand had caused the carboxy-terminal helices 11 and 12 of RAR to move over the bound retinoid in what the authors termed a "mouse-trap" mechanism. This change in structure may help to explain the biophysical changes observed upon ligand binding to a receptor. In the RAR and RXR, retinoid binding was accompanied by loss of greater than 90% of the tryptophan fluorescence signal (10, 11). This may result from trapping of the bound retinoid in close proximity to one or more tryptophan residues in the binding pocket. The relevance of these observations to the VDR is highlighted by sequence comparison. The amino acid sequences of the LBDs of the RAR, thyroid hormone receptor, and VDR were aligned using the program Pileup (Genetics Computer Group, University of Wisconsin-Madison). The solved structures of the TR and RAR showed a high degree of alignment of secondary structural elements and amino acids in contact with bound ligand (Fig. 10). The LBD of the VDR showed significant sequence matchup with the other receptors as shown by the alignment of identical residues between all three proteins. From this alignment, it can be extrapolated that the tryptophan residue in the VDR may be in a region of β-sheet (Fig. 10). This VDR tryptophan is in a sequence which in the RAR and TR contains residues in proximity to bound ligand (phenylalanine 288 in RAR and leucine 276 in TR). Our data shows that binding of 1,25-$(OH)_2D_3$ to the VDR resulted in tryptophan quenching of the same magnitude and mechanism as in the RXR and RAR, which suggests that the ligand and tryptophan may also be in close proximity in the VDR. This argument is supported by the near-UV CD spectrum (250–300 nm), which shows dramatic increases in signal upon addition of ligand. This CD signal arises from interactions of aromatic residue with their electronic environments, i.e., the details of the tertiary structure in vicinity of the residue (13). The increase in signal upon binding of ligand results from a significant change in the structure surrounding one or more aromatic residues. The major aromatic residue in this case could well be the

tryptophan; this is supported by preliminary results from mutagenesis studies where changing the tryptophan to a phenylalanine residue resulted in loss of half of the CD signal (S. Strugnell, D. McCaslin, and H. F. DeLuca, unpublished data). Taken together, these data support the idea that 1,25-$(OH)_2D_3$ binding significantly changes the conformation of the VDR LBD in the same manner as the RAR and TR. It is also likely that the ligand binds in close proximity to the tryptophan residue. However, in the absence of structure data this second conclusion must remain tentative.

In summary, the work presented in this paper shows that the LBD of the VDR can be expressed successfully in bacteria. Further research on crystallization of the LBD is required to determine the structure of the protein and from this the exact amino acids involved in ligand binding.

REFERENCES

1. Strugnell, S. A., and DeLuca, H. F. (1997) *Proc. Soc. Exp. Biol. Med.* **215,** 221–226.
2. Ross, T. K., Prahl, J. M., and DeLuca, H. F. (1991) *Proc. Natl. Acad. Sci. USA* **88,** 6555–6559.
3. Darwish, H. M., and DeLuca, H. F. (1996) *Prog. Nucl. Acid Res. Mol. Biol.* **53,** 321–344.
4. McDonnell, D. P., Scott, R. A., Kerner, S. A., O'Malley, B., and Pike, J. W., *et al.* (1989) *Mol. Endocrinol.* **3,** 635–644.
5. Bourguet, W., Ruff, M., Chambon, P., Gronemeyer, H., and Moras, D. (1995) *Nature* **375,** 377–382.
6. Renaud, J.-P., Rochel, N., Ruff, M., Vivat, V., Chambon, P., Gronemeyer, H., and Moras, D. (1995) *Nature* **378,** 681–689.
7. Wagner, R. L., Apriletti, J. W., McGrath, M. E., West, B. L., Baxter, J. D., and Fletterick, R. J. (1995) *Nature* **378,** 690–697.
8. Hörlein, A. J., Näär, A. M., Heinzel, T., Torchia, J., Gloss, B., Kurokawa, R., Ryand, A., Kamel, Y., Söderström, M., Glass, C. K., and Rosenfeld, M. G. (1995) *Nature* **377,** 397–404.
9. Perlmann, T., Umesono, K., Rangarajan, P. N., Forman, B. M., and Evans, R. M. (1996) *Mol. Endocrinol.* **10,** 958–966.
10. Lupiesella, J. A., Driscoll, J. E., Metzler, W. J., and Reczek, P. R. (1995) *J. Biol. Chem.* **270,** 24884–24890.
11. Bourguet, W., Ruff, M., Bonnier, D., Granger, F., Boeglin, M., Chambon, P., Moras, D., and Gronemeyer, H. (1995) *Prot. Express. Purif.* **6,** 604–608.
12. Cheng, L., Norris, A. W., Tate, B. F., Rosenberger, M., Grippo, J. F., and Li, E. (1994) *J. Biol. Chem.* **269,** 18661–18667.
13. Strickland, E. H. (1974) *CRC Crit. Rev. Biochem.* **2,** 113–175.
14. Apriletti, J. W., Baxter, J. D., Lau, K. H., and West, B. L. (1995) *Prot. Express. Purif.* **6,** 363–370.
15. Royer, C. A., Smith, W. R., and Beechem, J. M. (1991) *Anal. Biochem.* **192,** 287–294.
16. Royer, C. A., and Beechem, J. M. (1992) *Methods Enzymol.* **210,** 481–505.
17. Royer, C. A. (1993) *Anal. Biochem.* **210,** 91–97.
18. Smith, W. R., and Missen, R. W. (1982) Chemical Reaction Equilibrium Analysis, Wiley, New York.
19. Gratton, E., Limkemann, M., Lakowicz, J., Maliwal, B. P., Cherk, H., and Laczko, G. (1984) *Biophys. J.* **46,** 479–486.
20. Beechem, J. M., Gratton, E., Ameloot, M. A., Knutson, J. R., and Brand, L. (1992) *in* Topics in Fluorescence Spectroscopy (Lakowicz, J. R., Ed.), Vol. 2; pp. 241–301. Plum, New York.
21. Laue, T. M. (1995) *Methods Enzymol.* **259,** 427–452.
22. Cohn, E. J., and Edsall, J. T. (1943) *in* Proteins, Amino Acids, and Peptides, pp. 157–161, 370–375, Reinhold, New York.
23. Greenfield, N., and Fasman, G. D. (1969) *Biochemistry* **8,** 4108–4116.
24. Chen, Y.-H., Yang, J. T., and Martinez, H. M. (1972) *Biochemistry* **11,** 4120–4131.
25. Andrade, M. A., Chacón, P., Merelo, J. J., and Mordán, F. (1993) *Prot. Eng.* **6,** 383–390.
26. MacDonald, P. N., Haussler, C. A., Terpening, C. M., Galligan, M. A., Reeder, M. A., Whitfield, G. K., and Haussler, M. R. (1991) *J. Biol. Chem.* **266,** 18808–18813.
27. Strugnell, S. A., Wiefling, B. A., and DeLuca, H. F. (1995) *J. Bone Min. Res.* **10,** S396.
28. Craig, T. A., and Kumar, R. (1996) *Biochem. Biophys. Res. Commun.* **218,** 902–907.
29. Nakajima, S., Hsieh, J. C., MacDonald, P. N., Haussler, C. A., Galligan, M. A., Jurutka, P. W., and Haussler, M. R. (1993) *Biochem. Biophys. Res. Commun.* **197,** 478–485.
30. Chen, Z.-P., Shemshedini, L., Durand, B., Noy, N., Chambon, P., and Gronemeyer, H. (1994) *J. Biol. Chem.* **269,** 25770–25776.
31. Jehan-Kimmel, C., Jehan, F., and DeLuca, H. F. (1997) *Arch. Biochem. Biophys.* **341,** 75–80.
32. Cheskis, B., and Freedman, L. (1994) *Mol. Cell Biol.* **14,** 3329–3338.